Dynamic Characteristics Analysis and Stabilization of PV-Based Multiple Microgrid Clusters

Zhao, Zhuoli; Yang, Ping; Wang, Yuewu; Xu, Zhirong; Guerrero, Josep M.

Published in:
IEEE Transactions on Smart Grid

DOI (link to publication from Publisher):
10.1109/TSG.2017.2752640

Publication date:
2019

Document Version
Accepted author manuscript, peer reviewed version

Dynamic Characteristics Analysis and Stabilization of PV-Based Multiple Microgrid Clusters

Zhuoli Zhao, *Student Member, IEEE,* Ping Yang, *Member, IEEE,* Yuewu Wang, Zhirong Xu, *Student Member, IEEE,* and Josep M. Guerrero, *Fellow, IEEE*

***Abstract*—As the penetration of PV generation increases, there is a growing operational demand on PV systems to participate in microgrid frequency regulation. It is expected that future distribution systems will consist of multiple microgrid clusters. However, interconnecting PV microgrids may lead to system interactions and instability. To date, no research work has been done to analyze the dynamic behavior and enhance the stability of microgrid clusters considering the dynamics of the PV primary sources and dc links. To fill this gap, this paper presents comprehensive modeling, analysis, and stabilization of PV-based multiple microgrid clusters. A detailed small-signal model for PV-based microgrid clusters considering local adaptive dynamic droop control mechanism of the voltage-source PV system is developed. The complete dynamic model is then used to access and compare the dynamic characteristics of the single microgrid and interconnected microgrids. In order to enhance system stability of the PV microgrid clusters, a tie-line flow and stabilization strategy is proposed to suppress the introduced interarea and local oscillations. Robustly selecting of the key control parameters is transformed to a multiobjective optimization problem which is solved by genetic algorithm (GA). The proposed damping controller can effectively damp the power oscillations and provide robust control performance under variable operating conditions. Theoretical analysis, simulation results under various scenarios are presented to verify the effectiveness of the proposed scheme.**

***Index Terms*—Dynamic characteristics, photovoltaic (PV), multiple microgrid clusters, stability analysis, adaptive dynamic droop, stabilization.**

I. Introduction

In recent years, microgrids have experienced rapid development due to the advantages of reliability and flexibility compared with the conventional centralized power systems. Microgrids can integrate large amounts of renewable energy resources (RESs) and local loads to form low- and medium-voltage distributed power systems, thus gradually become an advanced architecture for future power supply and potentially a critical part of smart grid [1]–[3]. The isolating switch determines the operating modes of microgrids, i.e., grid-connected mode and autonomous mode, thus significantly improve reliability and power quality for the utility and customers [4].

With the increasing application of microgrids, it is expected that future distribution systems will consist of multiple microgrid clusters [5]. However, interconnecting microgrids may lead to system instability, which is not sufficiently investigated in current literature. This paper will study oscillations and stabilization of PV-based microgrid clusters.

A. Literature Review

1) Control approaches of microgrids

Typically, most distributed generations (DGs) are connected to the microgrids by using voltage source converters (VSCs). *P-f* and *Q-V* based droop control method is commonly employed to achieve adequate power sharing among DGs and ensure voltage and frequency stability [6]–[8]. The stability of droop-controlled microgrids has been studied in [9]–[11]. It is shown that the dominant low-frequency oscillatory modes are mainly associated with power sharing controllers. Several improved methods have been proposed in [12]–[14], in order to enhance the stability [12], remove the frequency and voltage deviations [13], and share harmonic loads power [14].

However, in the aforementioned literature, the possible fluctuations of the dc links connected to the converters are neglected [15], [16]. Moreover, the dynamic of the primary sources is relevant to RESs like photovoltaic (PV), where power fluctuations are inevitable due to the solar irradiation variations and corresponding maximum-power-point-tracking (MPPT) scheme [14], [17].

2) Contribution to frequency and voltage control by PV systems

The PV system converters are traditionally designed to deliver power to a utility grid. They can be represented as an ideal grid-connected current source [18]. Nevertheless, as the penetration of PV generation increases, reduced frequency response and regulation capability may result in severe frequency fluctuations under loads or irradiation disturbances. Therefore, there is a growing operational demand on PV systems to participate in microgrid frequency and voltage regulation.

PV systems can participate in the control of the microgrid frequency and voltage by means of current sources or voltage

This work was supported in part by the National High Technology Research and Development Program of China (863 Program-2014AA052001), by the Joint Ph.D. Scholarship of China Scholarship Council (201406150017), by the National Science and Technology Support Program (2015BAA06B02), by the Science and Technology Planning Project of Guangdong Province (2016B020245001), and by the Science and Technology Project of China Southern Power Grid Electric Power Research Institute (SEPRI-K143003).

Z. Zhao, P. Yang, Y. Wang and Z. Xu are with the School of Electric Power, South China University of Technology, Guangzhou 510640, China (e-mail: zhuoliscut@gmail.com; eppyang@scut.edu.cn; myth-pluto@163.com; 407849739@qq.com).

Z. Zhao is also with the Department of Electrical and Electronic Engineering, Imperial College, London SW7 2AZ, U.K. (e-mail: z.zhao@imperial.ac.uk).

J. M. Guerrero is with the Department of Energy Technology, Aalborg University, 9220 Aalborg, Denmark (e-mail: joz@et.aau.dk).

sources. In [19], an active power controller is introduced in order to curtail the PV power when the state of charge (SoC) of the energy storage system (ESS) exceeds the safe upper threshold. However, the technique in [19] does not allow PV systems to work alone in autonomous mode since PV converters are controlled as current sources. Voltage-source PV droop approaches have been proposed for PV converters to participate in frequency control directly in [20]–[22]. In [20] and [21], a hybrid PV controller is used to switch MPPT function and droop control under load transients. Nevertheless, the hybrid control scheme that switches between different configurations noticeably affects the stability and reliability of the PV system. Also, the two-stage converters are an expensive choice and lead to more power loss when multiple PV systems of rating in the range of few kW are adopted in residential microgrids. The usage of universal PV droop controller for single-stage PV inverters has been considered recently [22]. However, as will be revealed in this paper, the microgrid clusters stability will be challenged when using the proposed PV droop controller.

3) Interconnection of microgrids

In the event of output power variations caused by intermittent solar irradiation or failure of one or more DGs, single microgrid in islanded mode may not be secure enough to satisfy local load demand by the customers. In order to improve the security and reliability of power supply, neighboring microgrids can be interconnected to form multiple microgrid clusters. In this way, each microgrid can exchange power with its neighbors in the case of emergency situation.

Since the proposal of the microgrid clusters concept [23], [24], several related techniques on the control and operation of microgrid clusters have been introduced. Hierarchical and statistical energy management system are used to minimize the operational cost in [25] and [26], respectively. Multi-microgrids formation mechanism is proposed in [27] to restore critical loads after natural disaster caused faults in the main grid. In [28], distributed hierarchical control framework is presented to ensure reliable operation of dc interconnected microgrids. Nevertheless, the control framework in [28] only aims at dc microgrids, whereas this paper focuses on ac microgrids. Lately, the model order reduction analysis for microgrid clusters has been reported in [29] based on the theory of singularly perturbed systems. In [30]–[32], small signal stability of ideal inverter-based coupled microgrids is evaluated. Once again, however, the primary source dynamics of the DG units are ignored, and the dc voltages are assumed to be constant in [29]–[32].

B. Contribution

To date, no research work has been done to analyze the dynamic behavior and enhance the stability of microgrid clusters considering the dynamics of the PV primary sources and dc links. Furthermore, overall control and stabilization of the power flow in interconnected PV microgrids are still open to research.

Motivated by the aforementioned research gap, this paper presents comprehensive modeling, analysis, and stabilization of PV-based multiple microgrid clusters. A detailed small-signal model for PV-based microgrid clusters is developed. The model considers local adaptive dynamic droop control mechanism of the voltage-source PV system. The complete dynamic model is then used to access and compare the dynamic characteristics of the single microgrid and interconnected microgrids. This paper shows that the local mode and interarea mode in PV-based microgrid clusters can result in underdamped oscillatory behavior. As will be shown, interactions of PV microgrids might lead to power oscillations even if all PV sub-microgrids are individually stabilized. To stabilize the PV-based microgrid clusters, a tie-line flow and stabilization strategy is proposed to suppress the introduced local and interarea oscillatory modes. The proposed damping controller can effectively damp the power oscillations and provide robust control performance. Theoretical analysis, simulation results under various scenarios are presented to verify the effectiveness of the proposed strategy.

C. Paper Organization

The remainder of this paper is organized as follows. Section II gives the system configuration and characteristics of PV-based multiple microgrid clusters. After a general overview of conventional droop control, the proposed adaptive dynamic droop control scheme for PV-based sources is presented in Section III. Section IV presents dynamic modeling and stability analysis for the PV-based microgrid clusters. Section V discusses the tie-line flow and microgrid clusters stabilization strategy, as well as the optimal design of key parameters. Section VI shows the performance of the PV-based microgrid clusters in order to verify the stability analytical results and the proposed stabilization strategy. Finally, conclusion is given in Section VII.

II. Topology Architecture and Characteristics of PV-Based Multiple Microgrid Clusters

In consideration of increasing amounts of PV generations integrated into distribution network, Fig. 1 shows the single-line diagram and configuration of an exemplary PV-based multiple microgrid clusters. Since only islanded operation is considered in this work, the isolating switch S_1 is open. Thus all microgrids (i.e., MG 1, MG 2, and MG 3) are disconnected from the main grid. MG 1, MG 2, and MG 3 will be investigated in interconnected autonomous operation mode.

As shown in Fig. 1, microgrids are connected via resistive-inductive tie line, i.e., Tie line 1-2 and Tie line 2-3. Each microgrid is composed of two single-stage PV systems, one battery energy storage system (BESS) and local loads. All BESS units work in conventional droop controlled mode, while all PV systems operate in MPPT mode. Note that PV-based sources are capable of participating in frequency and voltage regulation through voltage-source adaptive dynamic droop control approach presented in Section III.

III. Adaptive Dynamic Droop Control Mechanism

A. Primary Droop Control for BESS

During microgrid autonomous mode, BESS unit operates as a grid supporting voltage source, which can achieve active and reactive power sharing in a decentralized manner. The controller of the BESS converter is composed of: 1) external power sharing control loop, which has responsibility to set the

This article has been accepted for publication in a future issue of this journal, but has not been fully edited. Content may change prior to final publication. Citation information: DOI 10.1109/TSG.2017.2752640, IEEE Transactions on Smart Grid

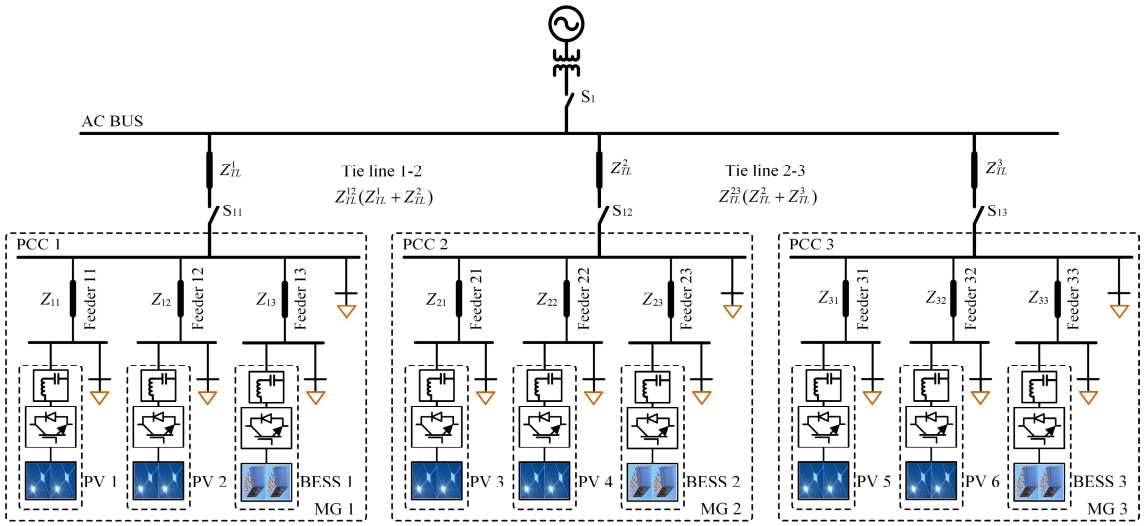

Fig. 1. Structure and configuration of the PV-based multiple microgrid clusters.

frequency and voltage magnitude for the output voltage of the inverter according to the droop characteristics; 2) voltage control loop, which is used to track the voltage reference; 3) inner current control loop to provide sufficient damping for the *LC* filter and limit transient overcurrent.

The principle of the conventional droop scheme allows BESS units to share active and reactive power by drooping corresponding frequency and voltage magnitude, respectively, and are given as follows:

$$\omega_{ES} = \omega_n^{ES} - m_P^{ES}(P_{ES} - P_{ES}^*) \quad (1)$$

$$V_{ES} = V_n^{ES} - n_Q^{ES}(Q_{ES} - Q_{ES}^*) \quad (2)$$

where ω_{ES} and V_{ES} are the output angular frequency and voltage magnitude reference of the BESS, ω_n^{ES} and V_n^{ES} are the set-point frequency and voltage, P_{ES} and Q_{ES} are the filtered active and reactive powers of the BESS, P_{ES}^* and Q_{ES}^* are corresponding references, and m_P^{ES} and n_Q^{ES} are the static active and reactive power droop coefficients, respectively.

B. Adaptive Dynamic Droop Control for PV-Based Sources

During grid-connected mode, PV generations are needed to track maximum power point (MPP) to deliver active/reactive power to local loads and utility grid. In autonomous mode, adaptive dynamic droop control for PV generation can provide flexible frequency and voltage support for the microgrids. According to low-load and high-load islanding operating conditions provided by the sub-microgrid central controller (SMGCC), deloaded voltage-source-based grid-supporting scheme and MPPT scheme can be adopted respectively. For simplicity, this study focuses on the worst-case scenario (high-load islanding). Thus, PV-based sources will operate in voltage-source MPPT scheme.

The control objectives and challenges in designing the adaptive dynamic droop PV inverter controller include: a) employ the droop concepts to achieve the function of autonomously controlling frequency and voltage and deloading solar generation in low-load islanding condition [22]; b) have MPPT capability for economic incentives; c) maintain the stability of the dc voltage during load transients and insolation variations.

1) Operating zone for PV-based sources

The P-V characteristics of the PV array for varying irradiance level are shown in Fig. 2(a). As discussed in [33], the dc-link voltage of the PV converter must satisfy the following criteria:

$$V_{DC} \geq 2\frac{V_{dq}}{D_{dq\_\max}} \quad (3)$$

with V_{dq} being the inverter output voltage in dq frame, $D_{dq\_\max}$ being the maximum modulating index in dq frame (i.e., $D_{dq\_\max} = 1$). Therefore, the design of the PV array must consider that the dc voltage of the MPP at a small irradiation level (say 0.05kW/m^2) meets the criteria of equation (3).

Fig. 2 shows that the stable operating zone of the PV system corresponds to the region that V_{DC} is higher than the MPP voltage, i.e., $dP_{PV}/V_{DC} < 0$, which will be considered in the design of adaptive droop scheme in Section III-B-2.

It should be noted that, in deloaded voltage-source-based grid-supporting scheme under low-load condition, the dc-link voltage is increased automatically through droop mechanism. Thus the active power is deloaded from its MPP power P_{MPP_n}. Once the PV system hits the MPPT when the microgrid load grows or the solar irradiation decreases, the dc-link voltage will be transferred to the MPP voltage such that the voltage-source MPPT scheme is activated.

2) Adaptive dynamic droop control

It is worth mentioning that the inertia of the PV system is the limited energy stored in the dc-link capacitor, which is usually around 0.01 pu-seconds of energy [34]. Therefore, the dc-link voltage may endure oscillations or collapse during load or solar irradiation transients. Fig. 3 presents the adaptive dynamic droop control scheme for PV-based sources [22]. In this diagram, the key part of dynamic droop control is the auxiliary dc-link voltage controller, which is supplemented to the active power droop control loop. In voltage-source MPPT scheme, this indicates that the output frequency of the PV systems will be adaptively adjusted through the auxiliary controller when the loads are suddenly increased or irradiation is sharply decreased. In this way, dc voltage can be preserved and load generation imbalance can

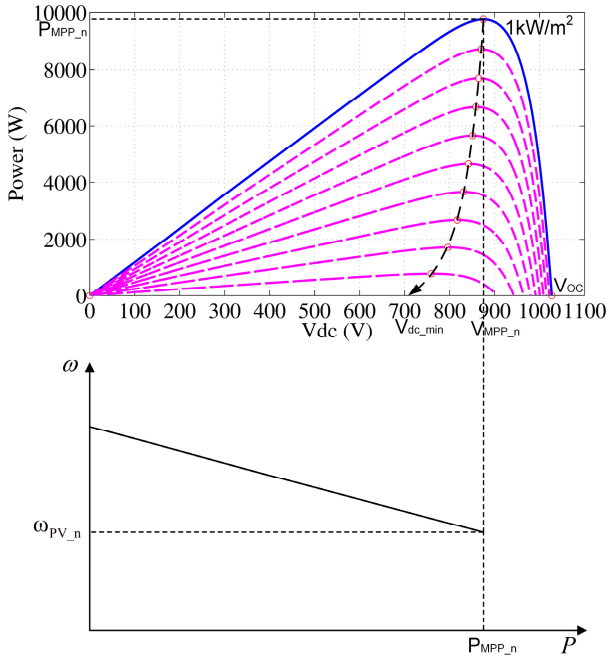

Fig. 2. Analysis of adaptive droop control of PV-based sources. (a) P-V curves of the PV array for varying irradiance level. (b) Corresponding droop characteristic.

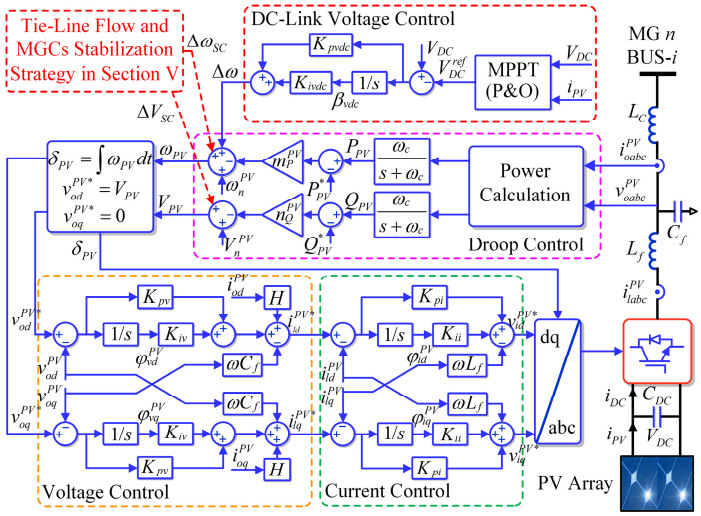

Fig. 3. Adaptive dynamic droop controller for the voltage-source PV system.

be compensated. As shown in Fig. 3, the outer loop of the adaptive dynamic droop control scheme can be expressed as follows:

$$\omega_{PV} = \omega_n^{PV} - m_P^{PV}(P_{PV} - P_{PV}^*) + K_{pvdc}(V_{DC} - V_{DC}^{ref}) + K_{ivdc}\int (V_{DC} - V_{DC}^{ref})dt \quad (4)$$

$$V_{PV} = V_n^{PV} - n_Q^{PV}(Q_{PV} - Q_{PV}^*) \quad (5)$$

where m_P^{PV} and n_Q^{PV} are the active and reactive power droop coefficients of the PV systems, K_{pvdc} and K_{ivdc} are the gains of the dc-link voltage controller, ω_n^{PV} and V_n^{PV} are the set-point frequency and voltage of the PV systems, P_{PV} and Q_{PV} are the filtered active and reactive powers of the PV systems, and P_{PV}^* and Q_{PV}^* are corresponding references, respectively.

Notice that, the reference of the dc-link voltage controller V_{DC}^{ref} is dynamically updated and regulated by the external MPPT controller. A perturb and observe (P&O) method is adopted in this work. Thus the voltage-source PV system can track MPP.

IV. Modeling and Stability Analysis

A. Dynamic Modeling for PV-Based Multiple Microgrid Clusters

The main objective of this section is to study the interactions and small-signal stability of the PV-based multiple microgrid clusters. Therefore, it is a crucial part to model and integrate the voltage-source PV-based system in the microgrid clusters. As shown in Fig. 3, the dynamic model of the PV-based unit is comprised of the sub-modules of the power circuit and control system, which are derived as follows.

Unlike the modeling of the ideal voltage-source inverter in [9], the dynamics of the PV array and the dc-link voltage are required to be considered in the plant model of the PV system. The PV array is mathematically described as function of current-voltage characteristic, as [35]

$$i_{PV} = N_p I_{ph} - N_p I_{rs}\left[\exp\left(\frac{qV_{DC}}{kT_T A_{IF} N_s N_c}\right) - 1\right] \quad (6)$$

where N_p and N_s are the number of parallel strings and series-connected modules per string, respectively; N_c is number of series-cells per module; I_{rs} is the diode reverse saturation current; I_{ph} is the short-circuit current of one string; q is the unit electric charge; k is Boltzman's constant; T_T is the p–n junction temperature (Kelvin); and A_{IF} is the ideality factor.

Dynamic of the dc link can be expressed based on the principle of power balance [36], [37]:

$$C_{DC}\frac{dV_{DC}}{dt} = i_{PV} - \frac{v_{id}^{PV} i_{ld}^{PV} + v_{iq}^{PV} i_{lq}^{PV}}{V_{DC}} \quad (7)$$

where C_{DC} is the dc-link capacitor, v_{id}^{PV} and v_{iq}^{PV} are the inverter-side output voltages of the PV system, and i_{ld}^{PV} and i_{lq}^{PV} are the output currents.

Thus, the power circuit dynamic can be modeled as follows:

$$\overbrace{\begin{bmatrix}\Delta\dot{V}_{DC}\\ \Delta\dot{i}_{ldq}^{PV}\\ \Delta\dot{v}_{odq}^{PV}\\ \Delta\dot{i}_{odq}^{PV}\end{bmatrix}}^{\Delta\dot{x}_{PC}^{PV}} = A_{PC}\overbrace{\begin{bmatrix}\Delta V_{DC}\\ \Delta i_{ldq}^{PV}\\ \Delta v_{odq}^{PV}\\ \Delta i_{odq}^{PV}\end{bmatrix}}^{\Delta x_{PC}^{PV}} + B_{PC1}\left[\Delta v_{idq}^{PV}\right] + B_{PC2}\left[\Delta v_{bdq}^{PV}\right] + B_{PC3}\left[\Delta\omega_{PV}\right] \quad (8)$$

In (8), Δv_{odq}^{PV}, Δi_{odq}^{PV} and Δv_{bdq}^{PV} are state variables of the PV output voltages (capacitor), PV grid-side output currents and bus voltages at the point of PV system connection, respectively. Note that the matrices A_{PC}, B_{PC1}, B_{PC2} and B_{PC3} can be obtained based on (7) and the dynamic model of the *LCL* filter.

In addition, based on equations (4) and (5), the state-space

This article has been accepted for publication in a future issue of this journal, but has not been fully edited. Content may change prior to final publication. Citation information: DOI 10.1109/TSG.2017.2752640, IEEE Transactions on Smart Grid

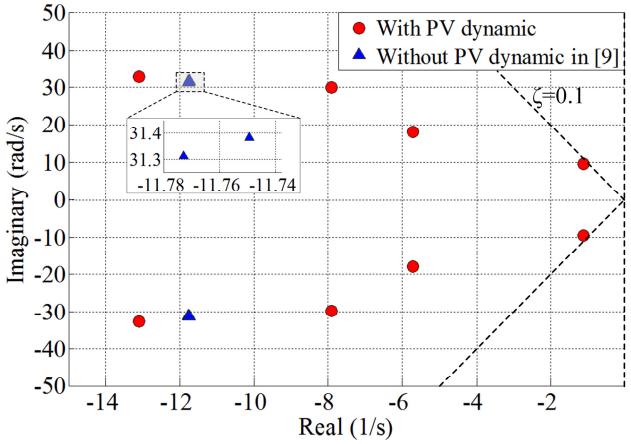

Fig. 4. Comparison of single area microgrid dominant modes with and without PV primary source dynamic (m_P^{PV}=4.7e^{-5}, K_{pvdc}=4e^{-4}, K_{ivdc}=5e^{-3}).

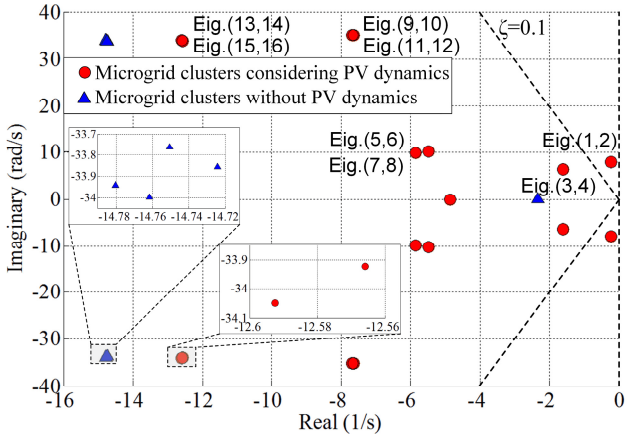

Fig. 5. Comparison of dominant modes of the multiple microgrid clusters considering PV dynamics and without considering PV dynamics in [29]–[32] (m_P^{PV}=4.7e^{-5}, K_{pvdc}=4e^{-4}, K_{ivdc}=5e^{-3}, TLL=250 m).

form of the outer loop of the adaptive dynamic droop controller can be given by

$$\begin{bmatrix}\Delta\omega_{PV}\\ \Delta v_{odq}^{PV*}\end{bmatrix}=\begin{bmatrix}C_{P\omega}^{PV}\\ C_{QV}^{PV}\end{bmatrix}\begin{bmatrix}\Delta\beta_{vdc}\\ \Delta\delta_{PV}\\ \Delta P_{PV}\\ \Delta Q_{PV}\end{bmatrix}+\begin{bmatrix}D_{P\omega}^{PV}\\ D_{QV}^{PV}\end{bmatrix}\begin{bmatrix}\Delta V_{DC}\\ \Delta i_{ldq}^{PV}\\ \Delta v_{odq}^{PV}\\ \Delta i_{odq}^{PV}\end{bmatrix} \tag{9}$$

where $\Delta\beta_{vdc}$ is the integrator state of the dc-link voltage controller; $\Delta\delta_{PV}$, ΔP_{PV}, and ΔQ_{PV} are the states of the droop controller; and superscript "$*$" denotes a reference value.

The dynamic models of the middle voltage controller and the inner current controller of the PV converter are derived with $\Delta\omega_{PV}$ and Δv_{odq}^{PV*} as inputs, and Δi_{ldq}^{PV*} and Δv_{idq}^{PV*} as outputs, given by

$$\dot{\left[\Delta\varphi_{vdq}^{PV}\right]}=A_V^{PV}\left[\Delta\varphi_{vdq}^{PV}\right]+B_{V1}^{PV}\left[\Delta v_{odq}^{PV*}\right]+B_{V2}^{PV}\Delta x_{PC}^{PV} \tag{10}$$

$$\left[\Delta i_{ldq}^{PV*}\right]=C_V^{PV}\left[\Delta\varphi_{vdq}^{PV}\right]+D_{V1}^{PV}\left[\Delta v_{odq}^{PV*}\right]+D_{V2}^{PV}\Delta x_{PC}^{PV} \tag{11}$$

$$\dot{\left[\Delta\varphi_{idq}^{PV}\right]}=A_C^{PV}\left[\Delta\varphi_{idq}^{PV}\right]+B_{C1}^{PV}\left[\Delta i_{ldq}^{PV*}\right]+B_{C2}^{PV}\Delta x_{PC}^{PV} \tag{12}$$

$$\left[\Delta v_{idq}^{PV*}\right]=C_C^{PV}\left[\Delta\varphi_{idq}^{PV}\right]+D_{C1}^{PV}\left[\Delta i_{ldq}^{PV*}\right]+D_{C2}^{PV}\Delta x_{PC}^{PV} \tag{13}$$

where $\Delta\varphi_{vdq}^{PV}$ and $\Delta\varphi_{idq}^{PV}$ are the state variables of the PV voltage and current controllers (the integrator states), respectively; Δx_{PC}^{PV} represents the states of the PV power circuit, as shown in (8).

Please note that in (9)–(13), the matrices $C_{P\omega}^{PV}$, C_{QV}^{PV}, $D_{P\omega}^{PV}$, D_{QV}^{PV}, A_V^{PV}, B_{V1}^{PV}, B_{V2}^{PV}, C_V^{PV}, D_{V1}^{PV}, D_{V2}^{PV}, A_C^{PV}, B_{C1}^{PV}, B_{C2}^{PV}, C_C^{PV}, D_{C1}^{PV} and D_{C2}^{PV} can be readily derived from the ODEs representing the droop, voltage and current controllers of the PV system.

Hence, the state-space model of ith PV-based system in the common reference frame can be developed by combining the dynamic models of the power circuit given in (8) and corresponding controllers given in (9)–(13), as follows:

$$\Delta\dot{x}_{PVi}=A_{PVi}\Delta x_{PVi}+B_{PVi}\Delta v_{bDQi}+B_{comi}\Delta\omega_{com} \tag{14}$$

$$\Delta x_{PVi}=\left[\Delta V_{DC}\quad \Delta i_{ldq}^{PV}\quad \Delta v_{odq}^{PV}\quad \Delta i_{odq}^{PV}\quad \Delta\beta_{vdc}\quad \Delta\delta_{PV}\quad \Delta P_{PV}\quad \Delta Q_{PV}\quad \Delta\varphi_{vdq}\quad \Delta\varphi_{idq}\right]^T \tag{15}$$

where $\Delta\omega_{com}$ is the frequency deviation of the common reference frame.

Now, the integrated dynamic model of the PV-based multiple microgrid clusters presented in Fig. 1 can be readily constructed as

$$\Delta\dot{x}_{MGC}=A_{MGC}\Delta x_{MGC} \tag{16}$$

$$\Delta x_{MGC}=[\underbrace{\Delta x_{PV1}\quad \Delta x_{PV2}\quad \Delta x_{ES1}\quad \Delta x_{NETj}\quad \Delta x_{LOADj}}_{\Delta x_{MG1}}\quad \underbrace{\cdots}_{\Delta x_{MGj}}\quad \underbrace{\Delta x_{TL}}_{\text{Tie Lines}}]^T \tag{17}$$

In (17), Δx_{MGj} is the states of jth PV microgrid; Δx_{ESi} is the states of the ith BESS unit; Δx_{NETj} and Δx_{LOADj} are the network states and the load states of the jth PV microgrid, respectively; and Δx_{TL} is states of the tie lines.

B. Stability Analysis

The derived dynamic model of (17) is then adopted to evaluate the small-signal stability of the proposed PV-based multiple microgrid clusters. The detailed system parameters are given in Tables I and II. To avoid excessive complexity, only two-area PV microgrid clusters are considered, thus to clearly investigate the dynamic characteristics of the microgrid clusters.

1) Impact of dynamics of the PV primary sources and dc links

First, the impact of the dynamics of the PV primary sources and dc links on microgrid stability is investigated. Fig. 4 compares dominant modes of single area microgrid with and without considering PV primary source and dc-link dynamics in (4) and (7), respectively. It can be seen that two pairs of low-frequency eigenvalues are yielded when considering PV dynamics and corresponding dc-link voltage controller.

In the case of multiple microgrid clusters, Fig. 5 shows the dominant modes of the microgrid clusters when considering the dynamics of the PV primary sources and without considering PV dynamics. As compared with the case ignoring primary source and dc-link dynamics in [29]–[32], several ultra-low-frequency and mid-low-frequency dominant modes are introduced in PV microgrid clusters. These critical modes yield more oscillatory system responses.

Therefore, it is found that ignoring the dynamics of the PV primary sources and assuming constant dc voltages for

This article has been accepted for publication in a future issue of this journal, but has not been fully edited. Content may change prior to final publication. Citation information: DOI 10.1109/TSG.2017.2752640, IEEE Transactions on Smart Grid

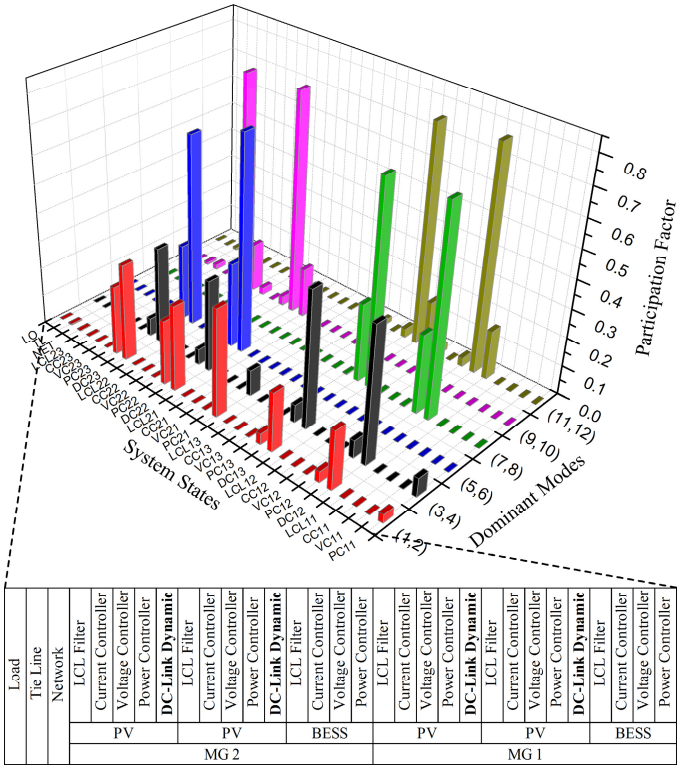

Fig. 6. Participation factor analysis (observability and controllability) of the state variables to dominant oscillatory modes of the PV multiple microgrid clusters with the parameters given in Table I.

simplicity in stability investigations of microgrid clusters may lead to misleading analytical results.

2) Participation factor analysis

Note that for two-area PV microgrid clusters, modeling and eigenvalue analysis show that the dimension of the system state matrix A_{MGC} in (16) is 106. The PV-based microgrid clusters system exhibits 48 pairs of complex-conjugate eigenvalues that correspond 48 oscillatory modes. Also, the system appears ten real negative eigenvalues. As can be seen in Fig. 5, the ultra-low-frequency and mid-low-frequency oscillatory modes are identified to be the dominant modes, which are crucial for system stability analysis. Please note that except the system dominant oscillatory modes corresponding to the dominant eigenvalues, all the other system modes are identified with high damping or high frequency of oscillation, which have negligible impact on microgrid system stability subsequent to a disturbance.

Participation matrix reflects observability and controllability of the state variables to the corresponding eigenvalues. In order to identify the correlation between system states and oscillatory modes of PV microgrid clusters, participation factor analysis is conducted. Fig. 6 presents the normalized participation factors of the microgrid state variables to the most dominant oscillatory modes (with damping less than -10 s^{-1}, i.e., Eigenvalues (1, 2), (3, 4), (5, 6), (7, 8), (9, 10) and (11, 12)).

As can be observed from Fig. 6, eigenvalues (1, 2), (3, 4), (5, 6), and (7, 8) represent the contributions of PV dynamics to microgrid clusters oscillations because these modes are noticeably participated by the state variables of the PV primary source and dc-link voltage controllers. Besides, eigenvalues (9, 10) and (11, 12) are attributed to the interactions of the power controllers of the PV units. Fig. 6

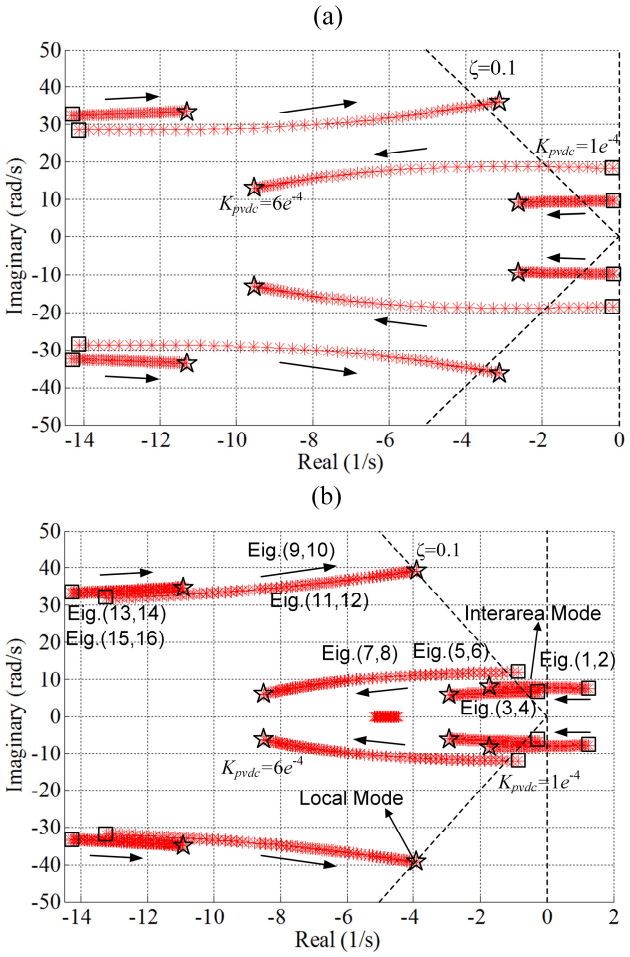

Fig. 7. Trajectory of microgrid dominant eigenvalues when the crucial control parameter K_{pvdc} is increased from 1e^{-4} to 6e^{-4} (m_P^{PV}=4.7e^{-5}, K_{ivdc}=5e^{-3}, TLL=250 m). (a) Single area PV-based microgrid. (b) PV-based multiple microgrid clusters.

shows that the states variables corresponding to the PV dynamics significantly contribute in most of the dominant modes. Therefore, the control parameters in (4) which describes the PV dynamics are selected as critical control parameters in the following sensitivity analysis.

3) Sensitivity analysis

In order to further examine the influence of interconnection of PV microgrids on the system stability, sensitivity analysis of the dominant eigenvalues to critical control and tie-line parameters is studied.

It is worth mentioning that the damping ratio (ζ) of all system oscillatory modes should be greater than a specified value. The minimum acceptable value of the damping ratio depends on sensitivity studies and system operating experience. Typically, ζ is in the range of 0.03 to 0.05 [38]. Besides, it is suggested that low-mid frequency oscillatory modes need better damping ratios (greater than 0.1) [39].

Fig. 7 shows the trajectory of dominant eigenvalues of single area and interconnected PV based microgrids, respectively, when the proportional gain of the dc-link voltage controller K_{pvdc} is increased from 1e^{-4} to 6e^{-4}. As can be seen from Fig. 7(a), proper value of K_{pvdc} can be selected to ensure sufficient damping ($\zeta = 0.1$) for the low-frequency oscillatory modes. However, when connecting the PV microgrids together, the microgrid clusters tend to occur

This article has been accepted for publication in a future issue of this journal, but has not been fully edited. Content may change prior to final publication. Citation information: DOI 10.1109/TSG.2017.2752640, IEEE Transactions on Smart Grid

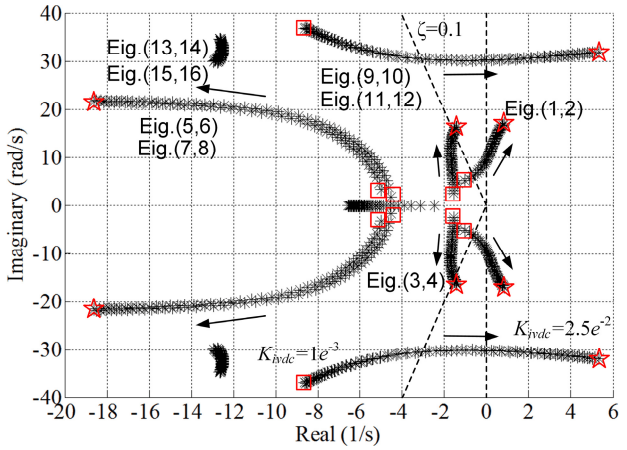

Fig. 8. Traces of the dominant modes of the PV multiple microgrid clusters for K_{ivdc} variations in the range of $1e^{-3}$ to $2.5e^{-2}$ (m_P^{PV}=4.7e^{-5}, K_{pvdc}=4e^{-4}, TLL=250 m).

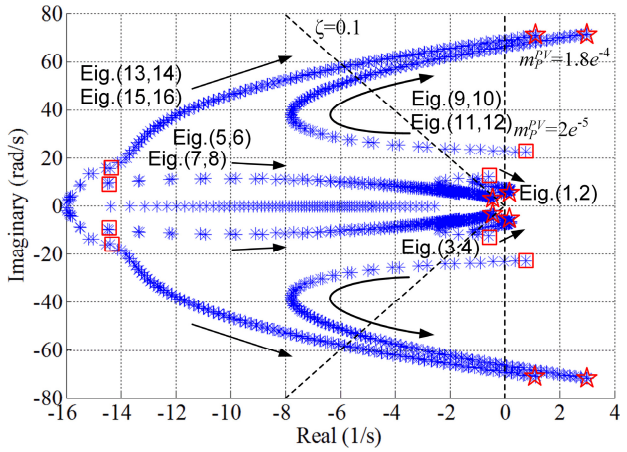

Fig. 9. Eigenvalue loci of the PV multiple microgrid clusters when increasing m_P^{PV} from $2e^{-5}$ to $1.8e^{-4}$ (K_{pvdc}=4e^{-4}, K_{ivdc}=5e^{-3},TLL=250 m).

ultra-low frequency oscillations (i.e., Eigenvalues (1, 2) and (3, 4), defined as interarea modes in this work) with a relatively small value of K_{pvdc}, as can be observed from Fig. 7(b). On the contrary, mid-low frequency oscillations (i.e., Eigenvalues (9, 10) and (11, 12), defined as local modes) might happen when choosing a relatively large value of K_{pvdc}.

Fig. 8 illustrates the traces of the dominant modes for the integral gain of the dc-link voltage controller K_{ivdc} variations in the range of $1e^{-3}$ to $2.5e^{-2}$. Fig. 8 shows that the damping ratios of the crucial modes (1, 2), (3, 4), (9, 10) and (11, 12) are decreased obviously. And eventually, these dominant modes cross to the right-hand plane (RHP) yielding to oscillatory responses.

The eigenvalue loci of the PV microgrid clusters when increasing the active power droop coefficient of the PV systems m_P^{PV} from $2e^{-5}$ to $1.8e^{-4}$ are shown in Fig. 9. Again, it can be observed that PV microgrid clusters have a general trend to excite ultra-low frequency and mid-low frequency oscillations.

Therefore, compared to the single area PV-based microgrid case in Fig. 7(a), it can be revealed that interconnecting neighboring PV microgrids remarkably reduces system damping and even destabilize the overall system due to the coupling of dominant oscillatory modes between neighboring microgrids.

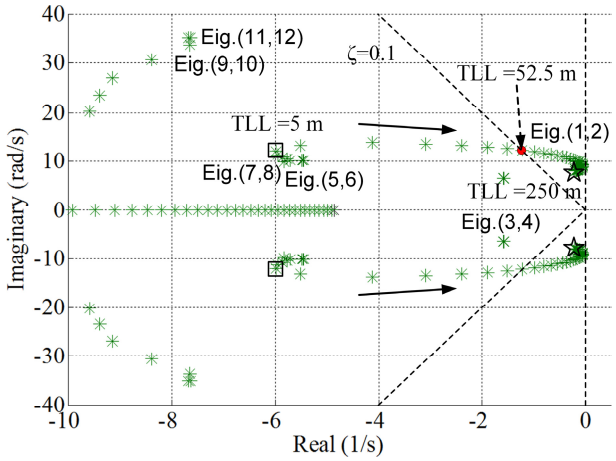

Fig. 10. Sensitivity of the PV multiple microgrid clusters dominant modes to variation of the tie line (connecting line) length TLL: 5 m ≤ TLL ≤ 250 m (m_P^{PV}=4.7e^{-5}, K_{pvdc}=4e^{-4}, K_{ivdc}=5e^{-3}).

When connecting microgrids, the system stability might be influenced by the electrical distance between microgrids. To analyze this effect, Fig. 10 illustrates the behavior of the dominant eigenvalues to variations of tie line (connecting line) length (TLL) in the range of 5 m to 250 m. It is shown that the critical TLL is identified as 52.5 m in which damping of the interconnected system can be guaranteed.

V. Tie-Line Power Flow Control and Multiple Microgrid Clusters Stabilization

A. Tie-Line Power Flow and Stabilization Control

As indicated by the small-signal stability and participation analysis, system damping of the PV based microgrid clusters is noticeably decreased by the PV dynamic and microgrids interconnection. Therefore, as shown in Fig. 3, to stabilize the PV multiple microgrid clusters, a tie-line power flow and microgrid clusters stabilization strategy is proposed to mitigate the introduced local and interarea oscillatory mode, given by

$$\Delta\omega_{SC} = K_{pSC}^{\omega}(\underbrace{K_{pSC}^{P}(P_{TLi}^{*} - P_{TLi})}_{\omega_{MGC}^{*}} - \omega_{MGC}) + K_{iSC}^{\omega}\int(\omega_{MGC}^{*} - \omega_{MGC})dt \quad (18)$$

$$\Delta V_{SC} = K_{pSC}^{V}(\underbrace{K_{pSC}^{Q}(Q_{TLi}^{*} - Q_{TLi})}_{V_{MGC}^{*}} - V_{MGC}) + K_{iSC}^{V}\int(V_{MGC}^{*} - V_{MGC})dt \quad (19)$$

where P_{TLi} and Q_{TLi} are the measured tie-line active and reactive power sent from SMGCC; P_{TLi}^{*} and Q_{TLi}^{*} are the desired tie-line active and reactive power; $\Delta\omega_{SC}$ and ΔV_{SC} are the supplementary terms; ω_{MGC} and V_{MGC} are the measured local microgrid frequency and voltage; K_{pSC}^{ω}, K_{iSC}^{ω}, K_{pSC}^{V} and K_{iSC}^{V} are the control parameters of the phase angle/frequency and voltage compensator; and K_{pSC}^{P} and K_{pSC}^{Q} are the control parameters of the power flow controller.

As can be seen in (18) and (19), when the PV microgrids are operating in interconnected mode, power flow control can be

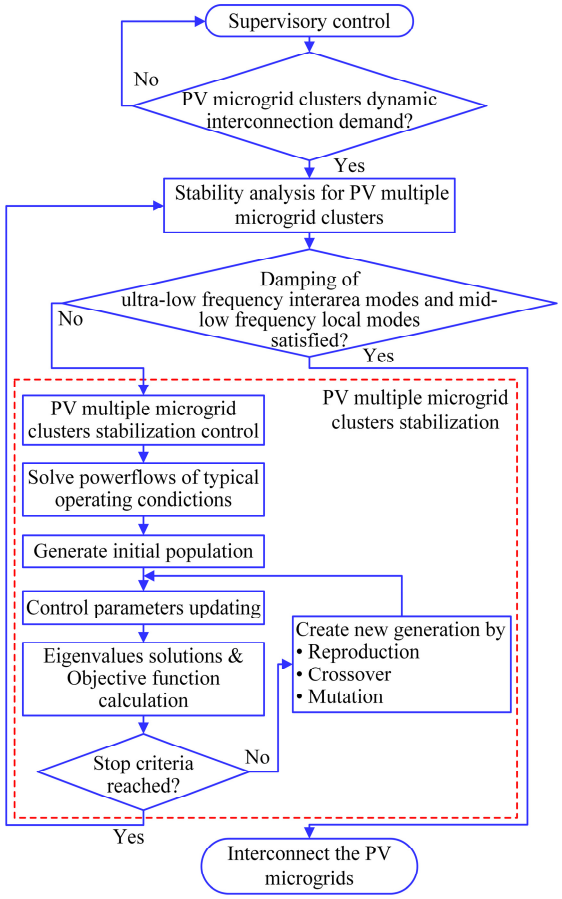

Fig. 11. Flowchart of the optimal design of PV multiple microgrid clusters stabilization control.

achieved by regulating the phase angle/frequency and voltage amplitude in the microgrid clusters. Thus, desired tie-line power P_{TLi}^{*} and Q_{TLi}^{*} can also be tracked. It is noted that by making the integral coefficients of the power flow controllers equal to zero, the tie-line control will perform as primary control of the PV microgrid clusters. In this way, single PV microgrid behaves as high-inertia voltage-source in interconnected mode.

B. Optimal Design of Stabilization Control Parameters

To enhance system damping characteristic of the PV microgrid clusters, the setting of the key control parameters is needed to optimize and coordinate. The selected objective function combining both damping factors and damping ratios can be formulated as

$$J=\sum_{i=1}^{N_p}\sum_{\zeta_{i,j}\le\zeta_o}(\zeta_o-\zeta_{i,j})^2+w\sum_{i=1}^{N_p}\sum_{\sigma_{i,j}\ge\sigma_o}(\sigma_o-\sigma_{i,j})^2 \qquad (20)$$

where N_p is the number of typical operating conditions, w is the weight of the multiple objective problem. The objective function (20) forms a stabilized region in which all damping ratios $\zeta_{i,j}$ and damping factors $\sigma_{i,j}$ are no less than ζ_o and no greater than σ_o, respectively.

Choosing microgrid clusters control parameters $\{K_{pSC}^{\omega}, K_{iSC}^{\omega}, K_{pSC}^{V}, K_{iSC}^{V}, K_{pSC}^{P}, K_{pSC}^{Q}, m_P^{PVi}, n_Q^{PVi}, K_{pvdci}, K_{ivdci}, m_P^{ESi}, n_Q^{ESi}\}$ as optimal variables, genetic algorithm (GA) is adopted to solve the optimization problem. Fig. 11 depicts the computational flowchart of the optimal design of PV microgrid clusters stabilization control. And the dominant

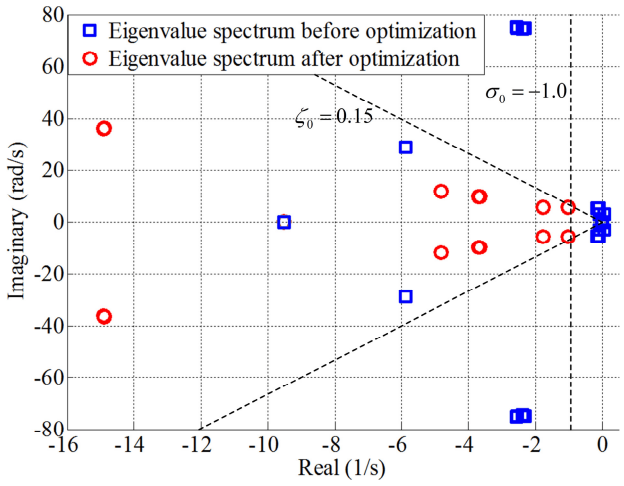

Fig. 12. Comparison of system eigenvalue spectrum before and after optimization (with the parameters given in Table I).

TABLE I
SYSTEM PARAMETERS OF THE MULTIPLE MICROGRID CLUSTERS

Parameter	Symbol	Value
Multiple microgrid clusters		
Grid voltage	V_g	380 V
Nominal frequency	f	50 Hz
Feeder impedance	$Z_{11}, Z_{12}, Z_{13}, Z_{21}, Z_{22}, Z_{23}$	$0.115+j0.05(\Omega)$
Tie-line impedance	Z_{TL}^{12}, Z_{TL}^{23}	$1.15+j0.5(\Omega)$ (250 m)
Power stage of the PV system		
DC-link voltage capacitor	C_{DC}	1000 μF
Output filter inductance	L_f	1.35 mH
Output filter capacitor	C_f	50 μF
Coupling inductance	L_C	0.35 mH
Switching frequency	f_S	8 kHz
PV adaptive dynamic droop controller (after optimization)		
Active power droop coefficient	m_P^{PV}	$4.7e^{-5}$
Reactive power droop coefficient	n_Q^{PV}	$1.3e^{-3}$
Proportional term of the dc-link voltage controller	K_{pvdc}	$3.55e^{-4}$
Integral term of the dc-link voltage controller	K_{ivdc}	$5e^{-3}$
Voltage and current controllers		
Proportional voltage term	K_{pv}	0.05
Integral voltage term	K_{iv}	390
Proportional current term	K_{pi}	10.5
Integral current term	K_{ii}	$16e^{3}$
Tie-Line power flow controller (after optimization)		
Proportional term of phase angle compensator	K_{pSC}^{ω}	0.05
Integral term of phase angle compensator	K_{iSC}^{ω}	10
Proportional term of voltage compensator	K_{pSC}^{V}	0.05
Integral term of voltage compensator	K_{iSC}^{V}	36
Proportional active power term	K_{pSC}^{P}	$2e^{-5}$
Proportional reactive power term	K_{pSC}^{Q}	$1.3e^{-3}$

eigenvalue spectrum of the PV microgrid clusters before and after optimization control are compared in Fig. 12. It is readily shown that the damping of the critical system low and mid-frequency oscillatory modes are significantly enhanced after optimization. This fact indicates that the PV microgrid clusters performance is in line with the design requirements.

This article has been accepted for publication in a future issue of this journal, but has not been fully edited. Content may change prior to final publication. Citation information: DOI 10.1109/TSG.2017.2752640, IEEE Transactions on Smart Grid

TABLE II
PV ARRAY PARAMETERS

Parameter	Value
PV array	$N_p = 2$, $N_s = 16$, $N_c = 96$, $I_{rs} = 1.1753e^{-8}$ A , $I_{ph} = 5.9602$ A , $q = 1.6022e^{-19}$ C , $k = 1.3806e^{-23}$ J/K , $T_T = 298$ K , $A_{IF} = 1.3$

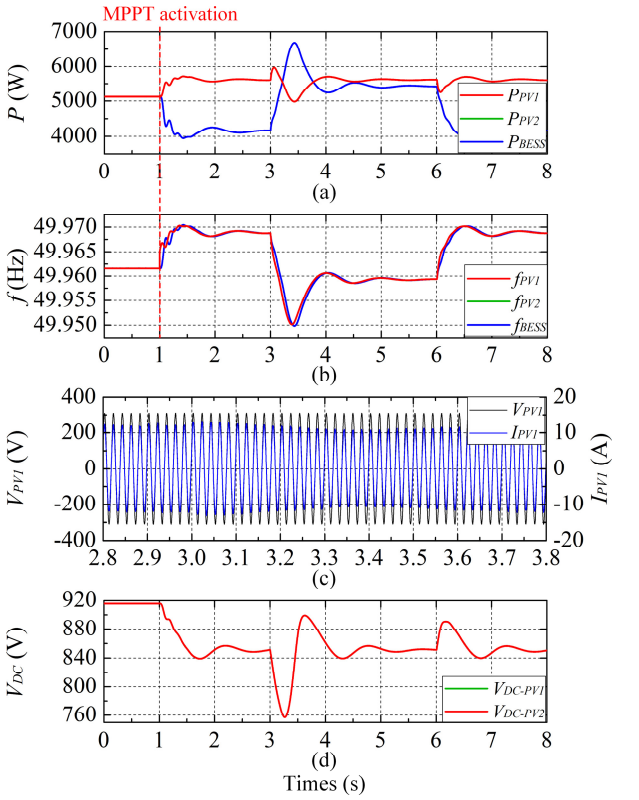

Fig. 13. Dynamic response of the PV single microgrid system with step load increase and decrease. (a) Active power. (b) Frequency. (c) Output current and voltage of PV 1. (d) DC voltage.

VI. SIMULATION RESULTS

In order to verify the preceding theoretical analysis presented in Section IV-B and evaluate the performance of the multiple microgrid clusters stabilization control scheme proposed in Section V, a 60 kVA PV-based multiple microgrid clusters composed of two identical microgrids is implemented under Matlab/Simulink environment. The main parameters of the PV multiple microgrid clusters are selected to be the same in both stability analysis and simulation, as listed in Tables I and II. Note that the parameters of *LCL* filter, voltage, current and power controllers of the BESS are identical with the PV system.

Various testing scenarios are provided to analyze the proposed system in the following sections.

A. Voltage-Source Operation of PV Systems

Fig. 13 shows the system response of the PV single microgrid when adopting adaptive dynamic droop control approach proposed in [22]. As can be seen, the voltage-source MPPT scheme is activated at $t = 1$ s , and the two PV systems both finally output maximum power of 5600 W. Then, a step load increase and decrease are applied to the microgrid at $t = 3$ s and $t = 6$ s , respectively. Fig. 13 shows that under load transients, the active power demand is shared properly among the PV systems and the BESS. Moreover, the output frequency of the PV systems are rapidly reduced through the adaptive dynamic droop control scheme presented in Section III-B-2. In this way, the extra load can be transferred to the BESS unit. Thus the dc voltage can be maintained and load generation imbalance can be effectively compensated.

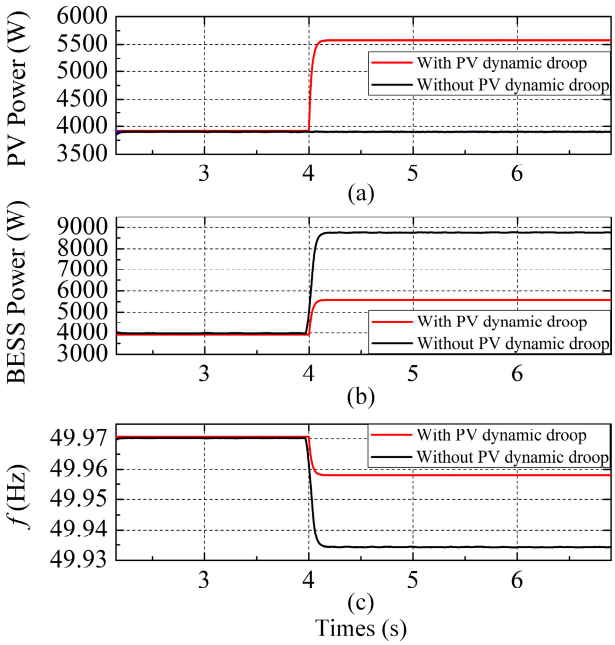

Fig. 14. Comparison of the PV single microgrid system response under step load increase with and without adopting adaptive dynamic droop control approach. (a) Active power of the PV systems. (b) Active power of the BESS. (c) Frequency.

Fig. 14 compares the dynamic performance of the single microgrid under step load increase of 4900 W with and without adopting adaptive dynamic droop control approach. Initially, all of the PV systems operate in the power dispatch mode with deload margin of 30%, providing in this way a 30 % generation reserve. When the load increases, the system frequency decreases and the PV systems adaptively increase their output active power to 5600 W according to the dynamic droop approach. However, conversely, the frequency regulation capability of the PV microgrid is relatively weak without adopting the PV dynamic droop scheme. Thus, the system frequency drops larger compared with the PV dynamic droop case.

It can be observed from Fig. 13 and Fig. 14 that the PV based sources are capable of participating in the regulation of microgrid frequency as autonomous voltage sources. Therefore, the control objectives of voltage-source control of PV inverters and corresponding MPPT capability have been achieved. Please note that this is significantly important in operation of PV microgrid when the penetration rate of photovoltaic is high.

B. Interaction and Instability Phenomena in PV Multiple Microgrid Clusters

In the case of microgrids interconnection, the performance of the PV microgrid clusters under a step load change of 1.8 kW in MG 1 is investigated, as presented in Fig. 15. Fig. 15(a) shows the active power of Tie line 1-2, whereas Fig. 15(c) depicts the system frequency of the two sub-microgrids. Note

This article has been accepted for publication in a future issue of this journal, but has not been fully edited. Content may change prior to final publication. Citation information: DOI 10.1109/TSG.2017.2752640, IEEE Transactions on Smart Grid

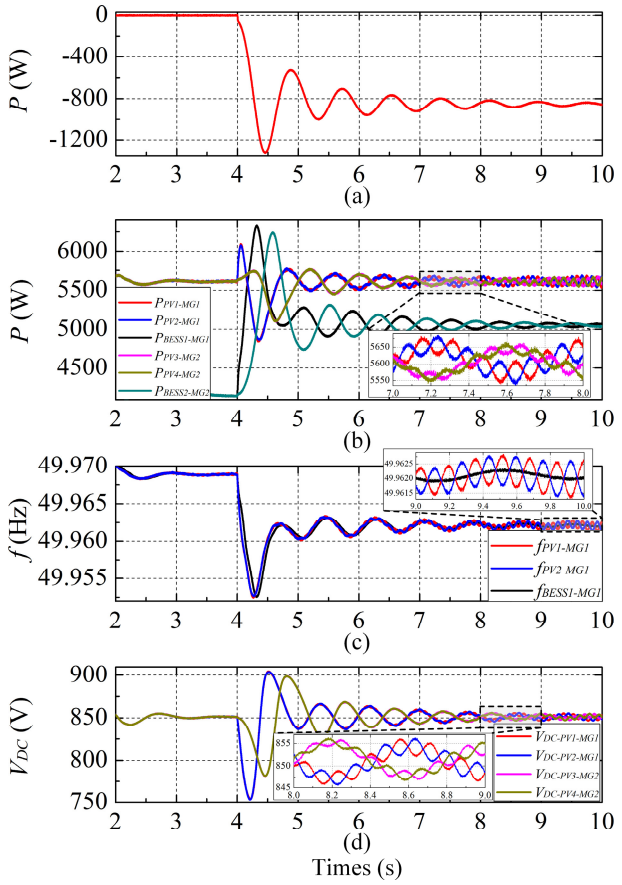

Fig. 15. Oscillations and instability phenomena of PV multiple microgrid clusters under 1.8 kW of step load change in MG 1. (a) Tie-line active power. (b) Active power of all DG units. (c) Frequency of MG 1. (d) DC voltage of the PV systems.

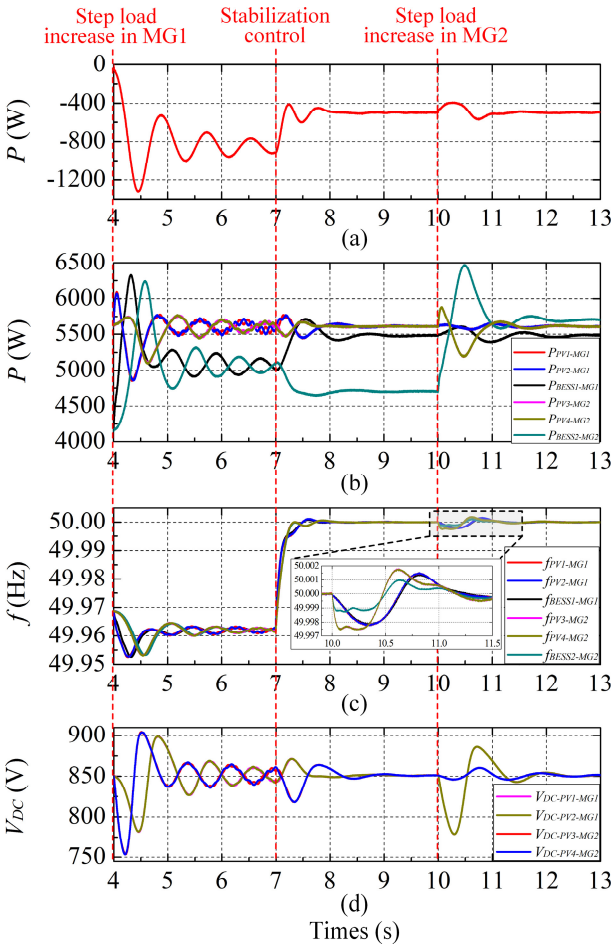

Fig. 16. System response of the PV multiple microgrid clusters under with tie-line power flow and stabilization control. (a) Tie-line active power. (b) Active power of all DG units. (c) Frequency. (d) DC voltage of the PV systems.

that all PV units initially operate in voltage-source MPPT mode.

As can be seen, when the load is stepped in a single area, the tie-line power oscillates with a frequency of 1.21 Hz, which is also reflected in the active power of the DG units and corresponding dc-link voltage of PV systems. These ultra-low-frequency oscillatory modes observed in tie line correspond to the interarea modes of PV microgrid clusters (i.e., Eig. (1, 2) and (3, 4)) predicted in small-signal stability analysis (see Fig. 7). The interarea modes are associated with the dynamics of PV primary source and dc voltage controllers.

Furthermore, as shown in Fig. 15(c) and (d), mid-low frequency oscillations are excited in the active power and dc voltage of the PV systems as a result of the step load increase. Moreover, the oscillations cannot be effectively mitigated even after 6 s. The frequency of these oscillations is around 5.88 Hz, which is consistent with the analytical finding of local modes (i.e., Eig. (9, 10) and (11, 12)) in PV microgrid clusters. It is worth noticing that since the local oscillatory modes only involve power swings between the PV systems in the sub-microgrids, the mid-low frequency oscillations cannot be observed in tie-line power.

Therefore, the presence of interactions among different PV sub-microgrids and different local PV systems remarkably reduce overall system damping. The oscillations have a negative effect on system dynamic performance and might lead to instability phenomena in PV based microgrid clusters.

C. Evaluation of Stabilization Control for PV Multiple Microgrid Clusters

The performance of the proposed PV multiple microgrid clusters stabilization strategy is tested in this section.

Fig. 16 presents the system dynamics under step load increase when tie-line power flow and stabilization control are activated. Comparing Fig. 16 with Fig. 15 clearly suggests the significant stable performance of the PV interconnected microgrids with the stabilization controller. As shown in Fig. 16, the damping controller can effectively suppress the ultra-low-frequency interarea oscillations and the mid-low frequency local oscillations under step load increase in MG 1 and MG 2 respectively, thus yielding highly damped power and frequency response. Note that the simulated results are again consistent with the theoretical analysis in Fig. 12.

Furthermore, in order to guarantee the satisfactory performance of the PV based microgrid clusters in the presence of PV power variations, the system response is examined under continuous solar irradiation fluctuations. Fig. 17 shows the system performance when the solar irradiation of all PV systems is continuously stepped down and stepped up. Note that considering the shading phenomena caused by the practical moving speed of the cloud, the solar irradiation variation of MG 2 lags behind that of MG 1, as shown in Fig. 17(b). As can be seen, all PV units initially are able to operate stably when voltage-source MPPT schemes are triggered at t =1.5 s. When the solar irradiation of the PV units decreases

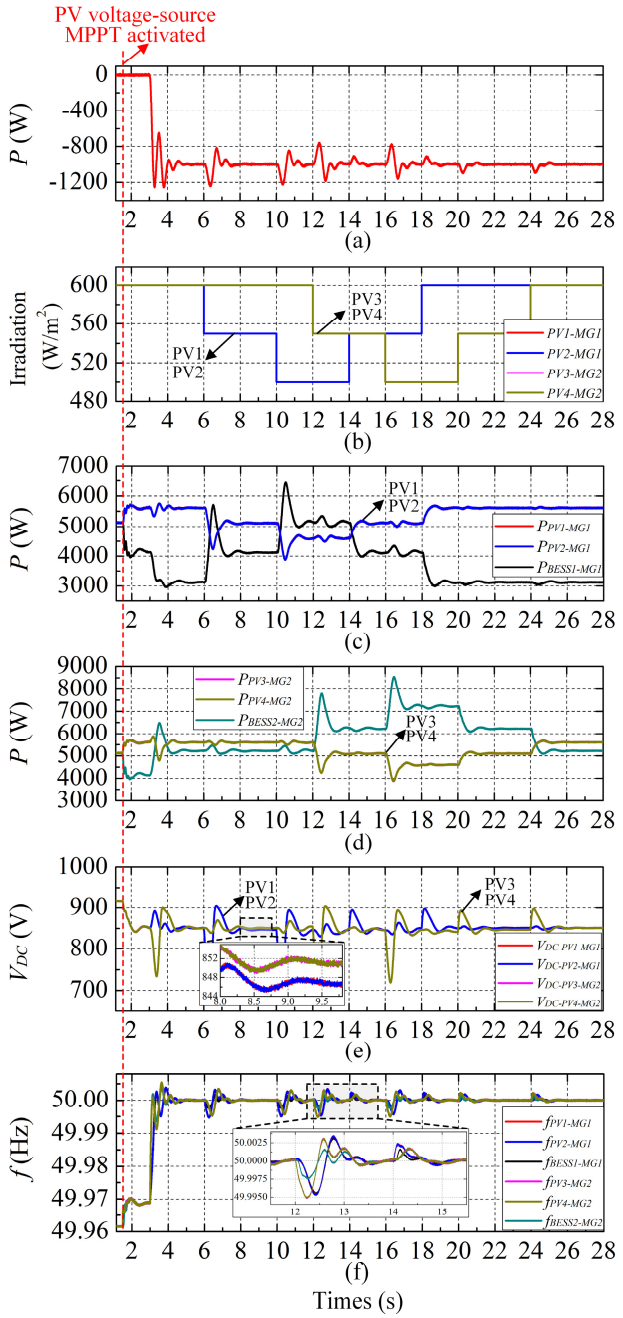

Fig. 17. Dynamic response of the PV multiple microgrid clusters with stabilization control in response to solar irradiation suddenly fluctuations. (a) Tie-line active power. (b) Solar irradiation of the PV systems. (c) Active power of the DG units in MG 1. (d) Active power of the DG units in MG 2. (e) DC voltage of all PV systems. (f) Frequency.

from 600 W/m^2 to 500 W/m^2 and then increases from 500 W/m^2 to 600 W/m^2, V_{DC}^{ref} can be dynamically updated by the MPPT controller, as shown in Fig. 17(e). Moreover, the output power and frequency of the PV systems can be adaptively regulated through the dynamic droop controller, as shown in Fig. 17(c), (d) and (f). Also, it can be observed from Fig. 17(a) and (c), during the solar irradiation fluctuation process, the proposed stabilization controller is capable of providing active damping characteristics to the PV multiple microgrid clusters. This behavior demonstrates the system performance is in line with the design requirements despite unexpected disturbances and variable operating conditions.

As the proposed tie-line power flow and stabilization control use low-bandwidth communication, failure of the

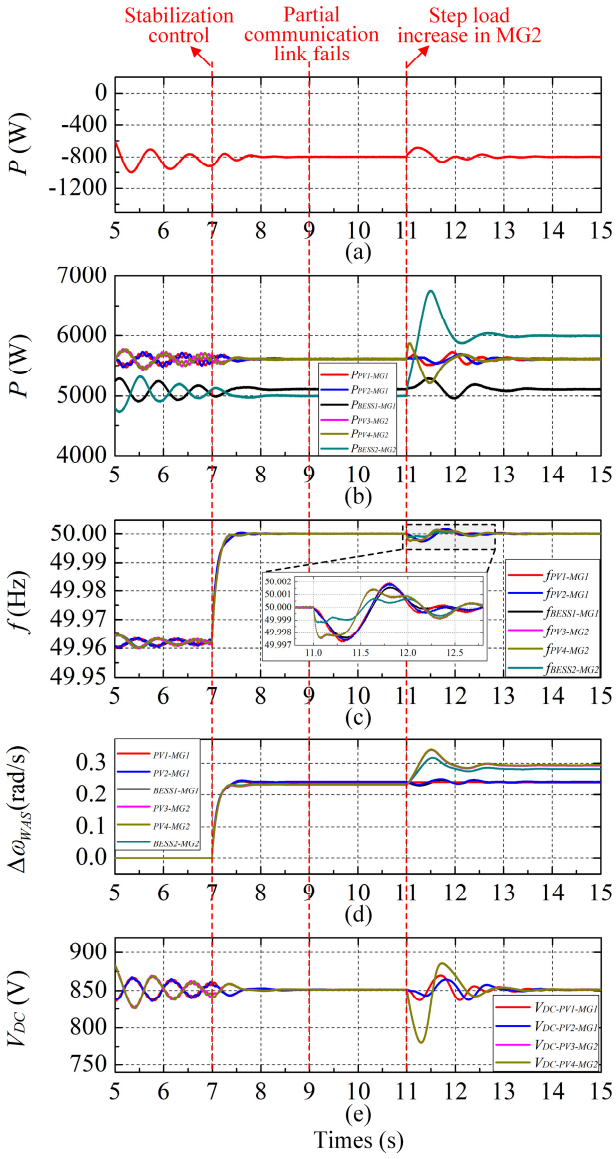

Fig. 18. Performance of the proposed tie-line power flow and stabilization control with partial communication link failure. (a) Tie-line active power. (b) Active power of all DG units. (c) Frequency. (d) Supplementary terms of all DG units. (e) DC voltage of the PV systems.

partial communication link may have an impact on system performance. The effectiveness of the controller is examined when assuming the communication link between SMGCC in MG 1 and PV 1 fails, and system performance is reported in Fig. 18. As shown in Fig. 18, tie-line power flow and stabilization control scheme is activated at t=7 s; the communication link between SMGCC of MG 1 and PV 1 is disconnected at t=9 s; then a step load increase of 1000 W is applied to MG 2 at t=11 s. Note that the measured tie-line active power P_{TLi} is locked to the value of the last time before the communication link fails. Thus the supplementary term of PV 1 remains the steady-state value unchanged, as can be seen from Fig. 18(d). Fig. 18 shows that the PV microgrid clusters can be effectively stabilized under step load change in MG 2 even though the communication channel has not yet been restored. Therefore, the proposed stabilization control scheme provides satisfactory reliability for PV microgrid clusters when partial communication link fails.

VII. Conclusion

This paper has addressed dynamic interactions, overall control, and stabilization in PV-based multiple microgrid clusters. A detailed small-signal model for PV-based multiple microgrid clusters considering local adaptive dynamic droop control mechanism of the voltage-source PV system is developed. Small-signal stability analysis shows that low-frequency eigenvalues are introduced when considering PV primary source dynamics and corresponding controllers. Furthermore, it is revealed that interconnecting neighboring PV microgrids yields ultra-low frequency interarea oscillations between sub-microgrids and mid-low frequency local oscillations behaviors within sub-microgrids. The interactions between PV microgrids significantly reduces system damping and leads to system instability.

In order to enhance system stability of the PV multiple microgrid clusters, a tie-line flow and stabilization strategy is proposed to suppress the introduced interarea and local oscillatory modes. Moreover, the problem of robustly choosing the key control parameters is then transformed to an eigenvalue-based multiobjective optimization problem which is solved by a genetic algorithm. The proposed stabilization control scheme shows robust performance despite unexpected disturbances and variable operating conditions, such as step load increase, continuous solar irradiation fluctuations and failure of the partial communication link. A theoretical analysis, simulation results under various scenarios have been presented to verify the finding of interactions and instability phenomena in PV multiple microgrid clusters and also the effectiveness of the proposed stabilization scheme.

References

[1] R. H. Lasseter, "Microgrids," in *Proc. IEEE Power Eng. Soc. Winter Meet.*, Jan. 2002, vol. 1, pp. 305–308.

[2] N. Hatziargyriou, H. Asano, R. Iravani, and C. Marnay, "Microgrids," *IEEE Power Energy Mag.*, vol. 5, no. 4, pp. 78–94, Jul. 2007.

[3] F. Katiraei, R. Iravani, N. Hatziargyriou, and A. Dimeas, "Microgrids management," *IEEE Power Energy Mag.*, vol. 6, no. 3, pp. 54–65, 2008.

[4] J. M. Guerrero, J. C. Vasquez, J. Matas, L. G. de Vicuña, and M. Castilla, "Hierarchical control of droop-controlled AC and DC microgrids—A general approach toward standardization," *IEEE Trans. Ind. Electron.*, vol. 58, no. 1, pp. 158–172, Jan. 2011.

[5] R. H. Lasseter, "Smart distribution: Coupled microgrids," *Proc. IEEE*, vol. 99, no. 6, pp. 1074–1082, Jun. 2011.

[6] M. C. Chandorkar, D. M. Divan, and R. Adapa, "Control of parallel connected inverters in standalone AC supply systems," *IEEE Trans. Ind. Appl.*, vol. 29, no. 1, pp. 136–143, Jan./Feb. 1993.

[7] J. M. Guerrero, M. Chandorkar, T. Lee, and P. C. Loh, "Advanced control architectures for intelligent microgrids—Part I: Decentralized and hierarchical control," *IEEE Trans. Ind. Electron.*, vol. 60, no. 4, pp. 1254–1262, Apr. 2013.

[8] Y. Han, H. Li, P. Shen, E. A. A. Coelho and J. M. Guerrero, "Review of active and reactive power sharing strategies in hierarchical controlled microgrids," *IEEE Trans. Power Electron.*, vol. 32, no. 3, pp. 27–51, 2017.

[9] N. Pogaku, M. Prodanovic, and T. C. Green, "Modeling, analysis and testing of autonomous operation of an inverter-based microgrid," *IEEE Trans. Power Electron.*, vol. 22, no. 2, pp. 613–625, Mar. 2007.

[10] J. M. Guerrero, J. C. Vasquez, J. Matas, M. Castilla, and L. G. de Vicuna, "Control strategy for flexible microgrid based on parallel line-interactive UPS systems," *IEEE Trans. Ind. Electron.*, vol. 56, no.3, pp. 726–736, 2009.

[11] Z. Zhao, P. Yang, J. M. Guerrero, Z. Xu, and T. C. Green, "Multiple-time-scales hierarchical frequency stability control strategy of medium-voltage isolated microgrid," *IEEE Trans. Power Electron.*, vol. 31, no. 8, pp. 5974–5991, Aug. 2016.

[12] R. Majumder, B. Chaudhuri, A. Ghosh, R. Majumder, G. Ledwich, and F. Zare, "Improvement of stability and load sharing in an autonomous microgrid using supplementary droop control loop," *IEEE Trans. Power Syst.*, vol. 25, no. 2, pp. 796–808, May 2010.

[13] J. Hu, J. Zhu, D. G. Dorrell, and J. M. Guerrero, "Virtual flux droop method—A new control strategy of inverters in microgrids," *IEEE Trans. Power Electron.*, vol. 29, no. 9, pp. 4704–4711, Sep. 2014.

[14] H. Han, X. Hou, J. Yang, J. Wu, M. Su and J. M. Guerrero, "Review of power sharing control strategies for islanding operation of AC microgrids," *IEEE Trans. Smart Grid*, vol. 7, no. 1, pp. 200–215, Jan. 2016.

[15] H. Liu, P. C. Loh, X. Wang, Y. Yang, W. Wang and D. Xu, "Droop control with improved disturbance adaption for a PV system with two power conversion stages," *IEEE Trans. Ind. Electron.*, vol.63, no.10,73–85, 2016.

[16] P. H. Divshali, A. Alimardani, S. H. Hosseinian and M. Abedi, "Decentralized cooperative control strategy of microsources for stabilizing autonomous VSC-based microgrids," *IEEE Trans. Power Syst.*, vol. 27, no. 4, pp. 1949–1959, Nov. 2012.

[17] M. A. G. de Brito, L. Galotto, L. P. Sampaio, G. d. A. e Melo and C. A. Canesin, "Evaluation of the main MPPT techniques for photovoltaic applications," *IEEE Trans. Ind. Electron.*, vol. 60, no.3, 1156–1167, 2013.

[18] J. Rocabert, A. Luna, F. Blaabjerg, and P. Rodríguez, "Control of power converters in AC microgrids," *IEEE Trans. Power Electron.*, vol. 27, no. 11, pp. 4734–4749, Nov. 2012.

[19] D. Wu, F. Tang, T. Dragicevic, J. C. Vasquez and J. M. Guerrero, "Autonomous active power control for islanded AC microgrids with photovoltaic generation and energy storage system," *IEEE Trans. Energy Convers.*, vol. 29, no. 4, pp. 882–892, Dec. 2014.

[20] A. Elrayyah, Y. Sozer, and M. Elbuluk, "Microgrid-connected PV-based sources: a novel autonomous control method for maintaining maximum power," *IEEE Ind. Appl. Mag.*, vol. 21, no. 2, pp. 19–29, Mar. 2015.

[21] A. Elrayyah, Y. Sozer, and M. E. Elbuluk, "Modeling and control design of microgrid-connected PV-based sources," *IEEE J. Emerg. Sel. Top. Power Electron.*, vol. 2, no. 4, pp. 907–919, 2014.

[22] W. Du, Q. Jiang, M. J. Erickson, and R. H. Lasseter, "Voltage-source control of PV inverter in a CERTS microgrid," *IEEE Trans. Power Deliv.*, vol. 29, no. 4, pp. 1726–1734, Aug. 2014.

[23] N. J. Gil and J. A. Peas Lopes, "Hierarchical frequency control scheme for islanded multi-microgrids operation," in *Power Tech, 2007 IEEE Lausanne*, 2007, pp. 473–478.

[24] EU More-Microgrids [Online]. Available: http://www.microgrids.eu

[25] P. Tian, X. Xiao, K. Wang, and R. Ding, "A hierarchical energy management system based on hierarchical optimization for microgrid community economic operation," *IEEE Trans. Smart Grid*, vol. 7, no. 5, pp. 2230–2241, Sep. 2016.

[26] M. Fathi and H. Bevrani, "Statistical cooperative power dispatching in interconnected microgrids," *IEEE Trans. Sustain. Energy*, vol. 4, no. 3, pp. 586–593, Jul. 2013.

[27] C. Chen, J. Wang, F. Qiu, and D. Zhao, "Resilient distribution system by microgrids formation after natural disasters," *IEEE Trans. Smart Grid*, vol. 7, no. 2, pp. 958–966, Mar. 2016.

[28] Q. Shafiee, T. Dragicevic, J. C. Vasquez, and J. M. Guerrero, "Hierarchical control for multiple DC-microgrids clusters," *IEEE Trans. Energy Convers.*, vol. 29, no. 4, pp. 922–933, 2014.

[29] I. P. Nikolakakos, H. H. Zeineldin, M. S. El-Moursi, and N. D. Hatziargyriou, "Stability evaluation of interconnected multi-inverter microgrids through critical clusters," *IEEE Trans. Power Syst.*, vol. 31, no. 4, pp. 3060–3072, Jul. 2016.

[30] F. Shahnia, "Stability and eigenanalysis of a sustainable remote area microgrid with a transforming structure," *Sustain. Energy Grids Netw.*, vol. 8, pp. 37–50, Dec. 2016.

[31] R. Majumder and G. Bag, "Parallel operation of converter interfaced multiple microgrids," *Int. J. Electr. Power Energy Syst.*, vol. 55, pp. 486–496, Feb. 2014.

[32] F. Shahnia and A. Arefi, "Eigenanalysis-based small signal stability of the system of coupled sustainable microgrids," *Int. J. Electr. Power Energy Syst.*, vol. 91, pp. 42–60, 2017.

[33] A. Yazdani and R. Iravani, *Voltage-Sourced Converters in Power Systems*. New York, NY, USA: Wiley, 2010.

[34] M. J. Erickson, T. M. Jahns, and R. H. Lasseter, "Comparison of PV inverter controller configurations for CERTS microgrid applications," in *2011 IEEE Energy Conversion Congress and Exposition*, 2011, pp. 659–666.

[35] A. Yazdani and P. P. Dash, "A control methodology and characterization of dynamics for a photovoltaic (PV) system interfaced with a distribution network," *IEEE Trans. Power Deliv.*, vol. 24, no. 3, pp. 1538–1551, 2009.

[36] S. Liu, P. X. Liu, and X. Wang, "Stochastic small-signal stability analysis of grid-connected photovoltaic systems," *IEEE Trans. Ind. Electron.*, vol. 63, no. 2, pp. 1027–1038, Feb. 2016.

[37] M. Fazeli, J. B. Ekanayake, P. M. Holland, and P. Igic, "Exploiting PV inverters to support local voltage—A small-signal model," *IEEE Trans. Energy Convers.*, vol. 29, no. 2, pp. 453–462, Jun. 2014.
[38] R. Farmer, "Power systems dynamics and stability," in *The Electric Power Engineering Handbook*, L. Grigsby, Ed. Boca Raton, FL: CRC, 2001.
[39] B. Pal and B. Choudhuri, *Robust Control in Power Systems*. New York, NY, USA: Springer, 2005.

Zhuoli Zhao (S'15) received his B.S. degree from South China University of Technology, Guangzhou, China, in 2010, where he is currently working towards the Ph.D. degree in electrical engineering in the National-Local Joint Engineering Laboratory for Wind Power Control and Integration Technology.

From October 2014 to December 2015, he was a Visiting Ph.D. Student (Sponsored Researcher) with the Control and Power Research Group, Department of Electrical and Electronic Engineering, Imperial College London, London, U.K. Since July 2017, he has been a Research Associate with the Smart Grid Research Laboratory, Electric Power Research Institute, China Southern Power Grid, Guangzhou, China. His research interests include microgrid stability and control, power electronic converters, smart grids, and distributed generation systems. He is an active reviewer for IEEE Transactions on Power Electronics, IEEE Transactions on Smart Grid, IEEE Transactions on Sustainable Energy and IEEE Transactions on Industry Applications.

Ping Yang (M'11) received her M.S. and Ph.D. degree in control theory and engineering from South China University of Technology, Guangzhou, China, in 1994 and 1998, respectively.

Currently, she is a Professor with the School of Electric Power at South China University of Technology. She is also the Director of National-Local Joint Engineering Laboratory for Wind Power Control and Integration Technology, and Key Laboratory of Clean Energy Technology of Guangdong Province. Her research interests include integration of renewable energy into power system, microgrid control and management, and prediction modeling for wind and solar power.

Yuewu Wang was born in Guangxi, China, in 1983. He received his B.S. degree in Instrument Science and Technology from Xi'an Jiaotong University, Xi'an, China, in 2006; and his M.S. degree in Electrical Engineering from Guangxi University, Nanning, China, in 2010. He is currently working toward his Ph.D. degree in Electrical Engineering at the South China University of Technology, Guangzhou, China. His current research interests include pulse width modulation techniques and grid-connected inverters.

Zhirong Xu (S'15) received his B.S. degree in power systems from South China University of Technology, Guangzhou, China, in 2013, where he is currently working towards the Ph.D. degree in electrical engineering.

His research interests include microgrid energy management system and smart grids.

Josep M. Guerrero (S'01–M'04–SM'08–F'15) received the B.S. degree in telecommunications engineering, the M.S. degree in electronics engineering, and the Ph.D. degree in power electronics from the Technical University of Catalonia, Barcelona, Spain, in 1997, 2000, and 2003, respectively.

Since 2011, he has been a Full Professor with the Department of Energy Technology, Aalborg University, Aalborg, Denmark, where he is responsible for the Microgrid Research Program. Since 2012, he has been a Guest Professor with the Chinese Academy of Science, Beijing, China, and the Nanjing University of Aeronautics and Astronautics, Nanjing, China. Since 2014, he has been the Chair Professor with Shandong University, Jinan, China. Since 2015, he has been a Distinguished Guest Professor with Hunan University, Changsha, China. Since 2016, he has been a Visiting Professor Fellow with Aston University, Birmingham, U.K., and a Guest Professor with the Nanjing University of Posts and Telecommunications, Nanjing. His current research interests include oriented to different microgrid aspects, including power electronics, distributed energy-storage systems, hierarchical and cooperative control, energy management systems, smart metering, and the Internet of Things for ac/dc microgrid clusters and islanded minigrids, and maritime microgrids for electrical ships, vessels, ferries, and seaports.

Dr. Guerrero was a recipient of the Best Paper Award of the IEEE TRANSACTIONS ON ENERGY CONVERSION during 2014–2015, the Best Paper prize of the IEEE-PES in 2015, and the Best Paper Award of the JOURNAL of POWER ELECTRONICS in 2016. In 2014, 2015, and 2016, he was awarded by Thomson Reuters as Highly Cited Researcher, and in 2015 he was elevated as IEEE Fellow for his contributions on "distributed power systems and microgrids". He was the Chair of the Renewable Energy Systems Technical Committee of the IEEE Industrial Electronics Society. He is an Associate Editor of the IEEE TRANSACTIONS ON POWER ELECTRONICS, the IEEE TRANSACTIONS ON INDUSTRIAL ELECTRONICS, and the IEEE INDUSTRIAL ELECTRONICS MAGAZINE, and the Editor of the IEEE TRANSACTIONS ON SMART GRID and the IEEE TRANSACTIONS ON ENERGY CONVERSION. He has been a Guest Editor of the IEEE TRANSACTIONS ON POWER ELECTRONICS Special Issues: Power Electronics for Wind Energy Conversion and Power Electronics for Microgrids, the IEEE TRANSACTIONS ON INDUSTRIAL ELECTRONICS SPECIAL Sections: Uninterruptible Power Supplies systems, Renewable Energy Systems, Distributed Generation and Microgrids, and Industrial Applications and Implementation Issues of the Kalman Filter, the IEEE TRANSACTIONS ON SMART GRID Special Issues: Smart DC Distribution Systems and Power Quality in Smart Grids, and the IEEE TRANSACTIONS ON ENERGY CONVERSION Special Issue on Energy Conversion in Next-Generation Electric Ships.